

A switching-based backstepping sliding mode control for space manipulator in presence of gravity variation^①

Liu Fucui (刘福才)^{②*}, Zhao Wenna*, Meng Lingcong*, Liu Shuo**

(* Key Laboratory of Industrial Computer Control Engineering of Hebei Province, Yanshan University, Qinhuangdao 066004, P. R. China)

(** Engineering Department, University of Sheffield, Sheffield, UK)

Abstract

A novel switching-based backstepping sliding mode control (SBSMC) scheme is devised for the space manipulator exposed to different gravity. With a view to distinct differences in dynamics properties when the operating condition of space manipulator changes, the space manipulator can be thought of as a system composed of two subsystems, the ground subsystem and the space subsystem. Two different types of backstepping sliding mode (BSM) controllers are designed, one is suited for the ground subsystem and the other is for the space one. The switching between two subsystems can be implemented automatically when the switching mechanism is triggered, and the controllers for their subsystems experience synchronous switching. In this way, the space manipulator always has good behaviors in trajectory tracking. Moreover, multi-Lyapunov functions are introduced to prove the stability of this switching approach. According to simulation results, the method constructed in this research has better performance in control precision and adaptability compared with proportional-derivative (PD) control.

Key words: space manipulator, microgravity, switching system, multi-Lyapunov functions, backstepping sliding mode control (BSMC)

0 Introduction

The space manipulator is now integral to various significant missions carried out in the space for its powerful and flexible capabilities^[1]. Exploring favorable control methods to improve the control precision of space manipulator turns out to be quite necessary.

To ensure that a space manipulator functions well in performing space missions, conducting simulation tests on the ground is an indispensable process. The first concern is how to improve the accuracy of simulation in microgravity environment since the fact that many issues such as friction, links flexibility and hinge clearance are all related to gravity cannot be ignored. To solve these problems, traditional ways include the drop tower^[2], parabolic flight^[3], air flotation^[4], buoyancy method^[5], suspension method^[6], and so on. Recent researchers have yielded a great many inspiring results. The possible application of planar air-bearing microgravity simulator has been studied for the orbital capture manoeuvre and experiments results show that this simulator can be used to verify some control methods and strategies^[7]. A calibration system con-

structed to simulate the microgravity environment can be able to counterbalance the impact of gravity upon the space manipulator^[8]. The combination between neutral buoyancy and electromagnetic to balance the gravity and simulate the microgravity has been proved to be effective on the tested-body and its simulation precision is higher than that of neutral buoyancy mechanism^[9]. Microgravity simulation systems introduced above are categorized into environment simulation, which, however, can't provide long-time and reliable microgravity environment. In view of this, the simulation of motor behavior is regarded as a favorable substitute for environment simulation^[10]. Therefore, a fuzzy adaptive robust control was developed for space manipulator with change of gravity from ground to space, where the fuzzy algorithm is designed to approximate the uncertainties of system, the approximation error is compensated by applying a robust control algorithm^[11]. However, the determination of fuzzy rules and membership functions are based on experience. Given the variation of friction characteristics in different gravity environments, an active disturbance rejection control (ADRC) was put forward, in which parti-

① Supported by Manned Space Preresearch Project (No. 2016040301) and the Natural Science Foundation of Hebei Province (No. F2019203505).

② To whom correspondence should be addressed. E-mail: lfc@ysu.edu.cn

Received on Oct. 9, 2020

cle swarm optimization was introduced to optimize parameters of ADRC^[12]. Nevertheless, if the error in ADRC at initial time is too large, the control system may confront the conflict between quickness and overshoot.

In this study, a switching-based backstepping sliding mode control (SBSMC) is developed for space manipulator. Switching control has extensive application background for complex robotic systems^[13-15] and the theory of multi-Lyapunov functions are often used in proving the stability of the switching system^[16]. In addition, sliding mode control is widely applied in the field of robotics for good robustness to system uncertainties while backstepping wins reputation for its characteristic to reduce design complexity of system^[17-19]. In the approach of SBSMC, two subsystems are constructed for the space manipulator, two different kinds of backstepping sliding mode (BSM) controllers are then designed for these two subsystems. The switching mechanism dependent on event is set to trigger the synchronous switch of the target subsystem and its corresponding controller. The strategy proposed in this paper combines the advantages of switching control and BSM control and shows high efficiency and strong robustness in trajectory tracking of the space manipulator against the change of gravity environments. The stability of the control scheme can be guaranteed by the aid of multi-Lyapunov functions.

This paper is organized as follows. Section 1 describes mathematical models for the space manipulator, and Section 2 offers the architecture of the proposed scheme. The stability of SBSMC for the space manipulator is proved in Section 3. Section 4 demonstrates the experiment results and Section 5 draws a conclusion.

1 System description

The following are assumptions made on the space manipulator system^[11] (as shown in Fig. 1).

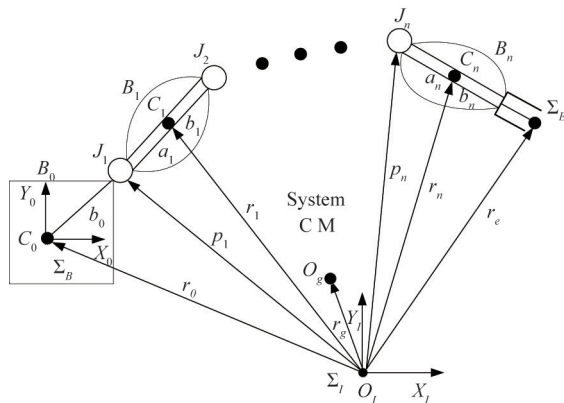


Fig. 1 free-floating space manipulator with *n*-DOF

Assumption 1 The system is a rigid body system.

Assumption 2 The system is composed of one base and *n* links. The pose of the base isn't active-controlled. Each joint of the link has one rotational degree of freedom (DOF) and is active-controlled.

1.1 Ground subsystem

During the tests on the ground, gravity has great influence on the behaviors of space manipulator and the Lagrange function is equal to the difference between kinetic energy and potential energy. Taking the effect of friction into consideration, the dynamic equation of the ground subsystem with fixed base derived from Lagrange equation is presented as

$$M(q)\ddot{q} + C(q, \dot{q})\dot{q} + G(q) + T_f = \tau \quad (1)$$

where $q \in \mathbf{R}^n$, \dot{q} , \ddot{q} are the joint position, velocity and acceleration, respectively; $M(q) \in \mathbf{R}^{n \times n}$ is the inertia matrix; $C(q, \dot{q}) \in \mathbf{R}^{n \times n}$ is the matrix composed of centrifugal force and coriolis force; $G(q) \in \mathbf{R}^n$ is the gravity matrix; $\tau \in \mathbf{R}^n$ is the driving torque exerted on the joints; $T_f \in \mathbf{R}^{n \times 1}$ denotes the friction torque vector^[12], in the gravity field, it is described as

$$T_f^{(i)} = \sum_{k=i}^n [G^{(k)} \cdot l_g^{(ki)} + F_t^{*(k)} \cdot l_t^{(ki)}] \quad (2)$$

where $T_f^{(i)}$ is the friction torque of the *i*th rotary joint; $G^{(k)}$ is the gravity load of the *k*th joint; $l_g^{(ki)}$ is the vertical dimension from the *i*th rotational axis to the gravity line of the *k*th joint's mass center; $F_t^{*(k)}$ is the tangential generalized inertia force of the *k*th joint and $l_t^{(ki)}$ is the vertical dimension from the *i*th rotational axis to the tangential generalized inertia force line of the *k*th joint's mass center.

1.2 Space subsystem

During the operation in the space, the motion of system increases 6-DOF as a result of a free-floating base. The Lagrange function is equal to the kinetic energy. Taking account of the influence of friction, the dynamic equation of the space subsystem derived from Lagrange equation is expressed as

$$M(q)\ddot{q} + C(q, \dot{q})\dot{q} + T_f = \tau \quad (3)$$

where $M(q) \in \mathbf{R}^{(n+6) \times (n+6)}$ is the inertia matrix, $C(q, \dot{q}) \in \mathbf{R}^{(n+6) \times (n+6)}$ is the matrix composed of centrifugal force and coriolis force. Denote the generalized displacement vector as $q = [q_b^T \quad q_m^T]^T \in \mathbf{R}^{n+6}$, where $q_b \in \mathbf{R}^6$ represents the pose vector of the base while $q_m = [q_1 \quad q_2 \quad \dots \quad q_n]^T \in \mathbf{R}^n$ reflects the generalized displacement vector of joints. Take $\tau = [0_{6 \times 1}^T \quad \tau_{n \times 1}^T]^T \in \mathbf{R}^{(n+6) \times 1}$ as the driving torque, where $0_{6 \times 1}$ signifies the driving torque of the base and $\tau_{n \times 1}$ means the driving

torque of joint. $\mathbf{T}_f = [\mathbf{0}_{6 \times 1}^T \quad \mathbf{T}_{fn \times 1}^T]^T \in \mathbf{R}^{n+6}$ describes the friction torque, here, it is expressed by

$$\mathbf{T}_f^{(i)} = \sum_{k=i}^n \mathbf{F}_t^{*(k)} \cdot l_t^{(ki)} \quad (4)$$

where $\mathbf{T}_f^{(i)}$ is the friction torque of the i th rotary joint; $\mathbf{F}_t^{*(k)}$ is the tangential generalized inertia force of the k th joint and $l_t^{(ki)}$ is the vertical dimension from the i th rotational axis to the tangential generalized inertia force line of the k th joint's mass center.

The following is one of characteristics of kinetic equation for the space manipulator^[20].

Property 1 $\mathbf{M}(\mathbf{q})$, which is bounded, is a positive definite symmetric matrix, i. e. ,

$$\lambda_m \|\boldsymbol{\eta}\|^2 \leq \boldsymbol{\eta}^T \mathbf{M}(\mathbf{q}) \boldsymbol{\eta} \leq \lambda_M \|\boldsymbol{\eta}\|^2, \quad \forall \boldsymbol{\eta} \in \mathbf{R}^{n+6}$$

where positive constants λ_m and λ_M are the minimum and maximum eigenvalues of $\mathbf{M}(\mathbf{q})$, respectively.

2 Design of SBSMC

Since the space manipulator involves two subsystems, namely, ground subsystem and space subsystem, two kinds of BSM controllers are required for these two subsystems. Originally, the debugging of space manipulator is carried out on the ground, thus the ground subsystem and its corresponding controller takes effect. As soon as the measuring instrument of gravity acceleration^[21] (which is installed in the spacecraft to exercise real-time monitoring of the gravity acceleration) detects that the gravity acceleration $\leq 10^{-4}$ g (g refers to acceleration of free fall), the control system switches from the ground subsystem to the space subsystem quickly, at the same time, the ground controller is replaced by the space one.

An adaptive law is adopted to estimate the disturbance $\boldsymbol{\omega}_i$ of i th ($i=1,2$) subsystem, and

$$\boldsymbol{\omega}_1 = \mathbf{G}(\mathbf{q}) + \mathbf{T}_f \quad (5)$$

$$\boldsymbol{\omega}_2 = \Delta \mathbf{M}(\mathbf{q}) \ddot{\mathbf{q}} + \Delta \mathbf{C}(\mathbf{q}, \dot{\mathbf{q}}) \dot{\mathbf{q}} + \mathbf{T}_f \quad (6)$$

where $\Delta \mathbf{M}(\mathbf{q})$ and $\Delta \mathbf{C}(\mathbf{q}, \dot{\mathbf{q}})$ are modeling error matrices of the space subsystem, what's more, $\Delta \mathbf{M}(\mathbf{q}, \dot{\mathbf{q}}) = \mathbf{M}(\mathbf{q}, \dot{\mathbf{q}}) - \mathbf{M}_0(\mathbf{q}, \dot{\mathbf{q}})$ and $\Delta \mathbf{C}(\mathbf{q}, \dot{\mathbf{q}}) = \mathbf{C}(\mathbf{q}, \dot{\mathbf{q}}) - \mathbf{C}_0(\mathbf{q}, \dot{\mathbf{q}})$, in which $\mathbf{M}_0(\mathbf{q})$ and $\mathbf{C}_0(\mathbf{q}, \dot{\mathbf{q}})$ represent nominal values of the dynamic model for space subsystem.

Therefore, Eqs(1) and (3) can be written as

$$\mathbf{M}_i(\mathbf{q}) \ddot{\mathbf{q}} + \mathbf{C}_i(\mathbf{q}, \dot{\mathbf{q}}) \dot{\mathbf{q}} = \boldsymbol{\tau}_i - \boldsymbol{\omega}_i \quad (7)$$

Assuming that the inverse of \mathbf{q} exists and from Property 1, Eq. (8) can be obtained.

$$\ddot{\mathbf{q}} = \mathbf{M}_i(\mathbf{q})^{-1} [\boldsymbol{\tau}_i - \boldsymbol{\omega}_i - \mathbf{C}_i(\mathbf{q}, \dot{\mathbf{q}}) \dot{\mathbf{q}}] \quad (8)$$

For the space manipulator subsystems described in Eq. (7), the main steps of BSM controllers are presen-

ted as follows.

Step 1 Define Lyapunov function V_{i1}

$$V_{i1} = \frac{1}{2} \boldsymbol{\varepsilon}_1^T \boldsymbol{\varepsilon}_1 \quad (9)$$

where $\boldsymbol{\varepsilon}_1$ is the position error and is defined by

$$\boldsymbol{\varepsilon}_1 = \mathbf{q} - \mathbf{q}_d \quad (10)$$

where \mathbf{q}_d is the desired joint position, and

$$\dot{\boldsymbol{\varepsilon}}_1 = \dot{\mathbf{q}} - \dot{\mathbf{q}}_d \quad (11)$$

$$\ddot{\boldsymbol{\varepsilon}}_1 = \ddot{\mathbf{q}} - \ddot{\mathbf{q}}_d \quad (12)$$

The virtual control $\boldsymbol{\alpha}_1$ is taken as

$$\boldsymbol{\alpha}_1 = \mathbf{c} \boldsymbol{\varepsilon}_1 \quad (13)$$

where $\mathbf{c} \in \mathbf{R}^{n \times n}$ is a positive definite symmetric constant matrix.

Construct the following equation

$$\boldsymbol{\varepsilon}_2 = \dot{\boldsymbol{\varepsilon}}_1 + \boldsymbol{\alpha}_1 = \dot{\mathbf{q}} - \dot{\mathbf{q}}_d + \mathbf{c} \boldsymbol{\varepsilon}_1 \quad (14)$$

Using Eqs(13) and (14), the derivative of V_{i1} becomes

$$\dot{V}_{i1} = \boldsymbol{\varepsilon}_1^T \dot{\boldsymbol{\varepsilon}}_1 = \boldsymbol{\varepsilon}_1^T \boldsymbol{\varepsilon}_2 - \boldsymbol{\varepsilon}_1^T \mathbf{c} \boldsymbol{\varepsilon}_1 \quad (15)$$

It can be derived from Eq. (15) that $\dot{V}_{i1} \leq 0$ so long as $\boldsymbol{\varepsilon}_2 = 0$.

Step 2 Another Lyapunov function V_{i2} is defined as

$$V_{i2} = V_{i1} + \frac{1}{2} \mathbf{s}^T \mathbf{s} \quad (16)$$

where \mathbf{s} is the sliding variable, which is set as

$$\mathbf{s} = \boldsymbol{\lambda}_1 \boldsymbol{\varepsilon}_1 + \boldsymbol{\varepsilon}_2 \quad (17)$$

where $\boldsymbol{\lambda}_1 \in \mathbf{R}^{n \times n}$ is a positive definite symmetric constant matrix.

The derivative of Eq. (14) holds the following equation

$$\dot{\boldsymbol{\varepsilon}}_2 = \ddot{\boldsymbol{\varepsilon}}_1 + \dot{\boldsymbol{\alpha}}_1 = \ddot{\mathbf{q}} - \ddot{\mathbf{q}}_d + \mathbf{c} \dot{\boldsymbol{\varepsilon}}_1 \quad (18)$$

Based on Eqs(14), (15) and (18), the derivative of V_{i2} is given by

$$\begin{aligned} \dot{V}_{i2} &= \dot{V}_{i1} + \mathbf{s}^T \dot{\mathbf{s}} \\ &= \boldsymbol{\varepsilon}_1^T \boldsymbol{\varepsilon}_2 - \boldsymbol{\varepsilon}_1^T \mathbf{c} \boldsymbol{\varepsilon}_1 + \mathbf{s}^T [\ddot{\mathbf{q}} - \ddot{\mathbf{q}}_d + \boldsymbol{\lambda}_1 (\boldsymbol{\varepsilon}_2 - \mathbf{c} \boldsymbol{\varepsilon}_1) + \mathbf{c} \dot{\boldsymbol{\varepsilon}}_1] \end{aligned} \quad (19)$$

Substituting Eq. (8) into Eq. (19), yields

$$\begin{aligned} \dot{V}_{i2} &= \dot{V}_{i1} + \mathbf{s}^T \dot{\mathbf{s}} \\ &= \boldsymbol{\varepsilon}_1^T \boldsymbol{\varepsilon}_2 - \boldsymbol{\varepsilon}_1^T \mathbf{c} \boldsymbol{\varepsilon}_1 + \mathbf{s}^T [\mathbf{M}_i(\mathbf{q})^{-1} (\boldsymbol{\tau}_i - \boldsymbol{\omega}_i \\ &\quad - \mathbf{C}_i(\mathbf{q}, \dot{\mathbf{q}}) \dot{\mathbf{q}}) - \ddot{\mathbf{q}}_d + \boldsymbol{\lambda}_1 (\boldsymbol{\varepsilon}_2 - \mathbf{c} \boldsymbol{\varepsilon}_1) + \mathbf{c} \dot{\boldsymbol{\varepsilon}}_1] \end{aligned} \quad (20)$$

Step 3 For each space manipulator subsystem, Lyapunov function is chosen as

$$V_i = V_{i2} + \frac{1}{2\chi} \tilde{\boldsymbol{\omega}}_i^T \tilde{\boldsymbol{\omega}}_i \quad (21)$$

where $\chi > 0$ and $\tilde{\boldsymbol{\omega}}_i$ represents the estimation error. Assume that the estimated value of $\boldsymbol{\omega}_i$ is $\hat{\boldsymbol{\omega}}_i$ and the disturbance is slow time-varying, i. e. , $\dot{\boldsymbol{\omega}}_i = 0$, then $\tilde{\boldsymbol{\omega}}_i$ and its derivative are expressed as

$$\tilde{\boldsymbol{\omega}}_i = \boldsymbol{\omega}_i - \hat{\boldsymbol{\omega}}_i \quad (22)$$

$$\dot{\tilde{\boldsymbol{\omega}}}_i = -\dot{\hat{\boldsymbol{\omega}}}_i \quad (23)$$

According to Eqs(20), (22) and (23), the derivative of V_i can be obtained as follows.

$$\begin{aligned} \dot{V}_i &= \dot{V}_{i2} + \frac{1}{\chi} \tilde{\omega}_i^T \dot{\tilde{\omega}}_i \\ &= \boldsymbol{\varepsilon}_1^T \boldsymbol{\varepsilon}_2 - \boldsymbol{\varepsilon}_1^T \mathbf{c} \boldsymbol{\varepsilon}_1 + \mathbf{s}^T [\boldsymbol{\lambda}_1 (\boldsymbol{\varepsilon}_2 - \mathbf{c} \boldsymbol{\varepsilon}_1) \\ &\quad + \mathbf{M}_i^{-1}(\mathbf{q}) (\boldsymbol{\tau}_i - \mathbf{C}_i(\mathbf{q}, \dot{\mathbf{q}}) \dot{\mathbf{q}} - \boldsymbol{\omega}_i) - \ddot{\mathbf{q}}_d \\ &\quad + \mathbf{c} \dot{\boldsymbol{\varepsilon}}_1] - \frac{1}{\chi} \tilde{\omega}_i^T \dot{\tilde{\omega}}_i - \mathbf{s}^T \mathbf{M}_i^{-1}(\mathbf{q}) \tilde{\omega}_i \end{aligned} \quad (24)$$

In virtue of $\mathbf{s}^T \mathbf{M}_i^{-1}(\mathbf{q}) \tilde{\omega}_i = (\mathbf{s}^T \mathbf{M}_i^{-1}(\mathbf{q}) \tilde{\omega}_i)^T = \tilde{\omega}_i^T (\mathbf{M}_i^{-1}(\mathbf{q}))^T \mathbf{s}$, Eq. (24) will be transformed into

$$\begin{aligned} \dot{V}_i &= \dot{V}_{i2} + \frac{1}{\chi} \tilde{\omega}_i^T \dot{\tilde{\omega}}_i \\ &= \boldsymbol{\varepsilon}_1^T \boldsymbol{\varepsilon}_2 - \boldsymbol{\varepsilon}_1^T \mathbf{c} \boldsymbol{\varepsilon}_1 + \mathbf{s}^T [\boldsymbol{\lambda}_1 (\boldsymbol{\varepsilon}_2 - \mathbf{c} \boldsymbol{\varepsilon}_1) \\ &\quad + \mathbf{M}_i^{-1}(\mathbf{q}) (\boldsymbol{\tau}_i - \mathbf{C}_i(\mathbf{q}, \dot{\mathbf{q}}) \dot{\mathbf{q}} - \hat{\boldsymbol{\omega}}_i) \\ &\quad - \ddot{\mathbf{q}}_d + \mathbf{c} \dot{\boldsymbol{\varepsilon}}_1] - \frac{1}{\chi} \tilde{\omega}_i^T (\dot{\tilde{\omega}}_i + \chi (\mathbf{M}_i^{-1}(\mathbf{q}))^T \mathbf{s}) \end{aligned} \quad (25)$$

The adaptive law of disturbance is depicted by

$$\dot{\hat{\boldsymbol{\omega}}}_i = -\chi (\mathbf{M}_i^{-1}(\mathbf{q}))^T \mathbf{s} \quad (26)$$

Hence, Eq. (25) can be described as

$$\dot{V}_i = \dot{V}_{i2} + \frac{1}{\chi} \tilde{\omega}_i^T \dot{\tilde{\omega}}_i$$

$$\begin{aligned} &= \boldsymbol{\varepsilon}_1^T \boldsymbol{\varepsilon}_2 - \boldsymbol{\varepsilon}_1^T \mathbf{c} \boldsymbol{\varepsilon}_1 + \mathbf{s}^T [\boldsymbol{\lambda}_1 (\boldsymbol{\varepsilon}_2 - \mathbf{c} \boldsymbol{\varepsilon}_1) \\ &\quad + \mathbf{M}_i^{-1}(\mathbf{q}) (\boldsymbol{\tau}_i - \mathbf{C}_i(\mathbf{q}, \dot{\mathbf{q}}) \dot{\mathbf{q}} - \hat{\boldsymbol{\omega}}_i) - \ddot{\mathbf{q}}_d + \mathbf{c} \dot{\boldsymbol{\varepsilon}}_1] \end{aligned} \quad (27)$$

The following is the control law formulated for each subsystem:

$$\boldsymbol{\tau}_i = \boldsymbol{\tau}_{ieq} + \boldsymbol{\tau}_{is} \quad (28)$$

where, $\boldsymbol{\tau}_{ieq}$ is the equivalent control law while $\boldsymbol{\tau}_{is}$ stands for the sliding mode control rule, they are computed by

$$\boldsymbol{\tau}_{ieq} = \mathbf{M}_i(\mathbf{q}) [-\boldsymbol{\lambda}_1 (\boldsymbol{\varepsilon}_2 - \mathbf{c} \boldsymbol{\varepsilon}_1) + \ddot{\mathbf{q}}_d - \mathbf{c} \dot{\boldsymbol{\varepsilon}}_1 - \mathbf{h} \mathbf{s}] + \mathbf{C}_i(\mathbf{q}, \dot{\mathbf{q}}) \dot{\mathbf{q}} + \hat{\boldsymbol{\omega}}_i \quad (29)$$

$$\boldsymbol{\tau}_{is} = -\rho \mathbf{M}_i(\mathbf{q}) \mathbf{h} \tanh(\mathbf{s}) \quad (30)$$

where, ρ is a positive constant, $\mathbf{h} \in \mathbf{R}^{n \times n}$ is a positive definite diagonal coefficient matrix and $\tanh(\cdot)$ is a hyperbolic tangent function, which satisfies

$$\tanh(s) = \begin{cases} [-1, 0) & s < 0 \\ [0, 1] & s \geq 0 \end{cases} \quad (31)$$

The control scheme projected in this article for space manipulator is shown in Fig. 2. Fig. 3 reveals the structure of BSM controller designed for the space manipulator subsystem.

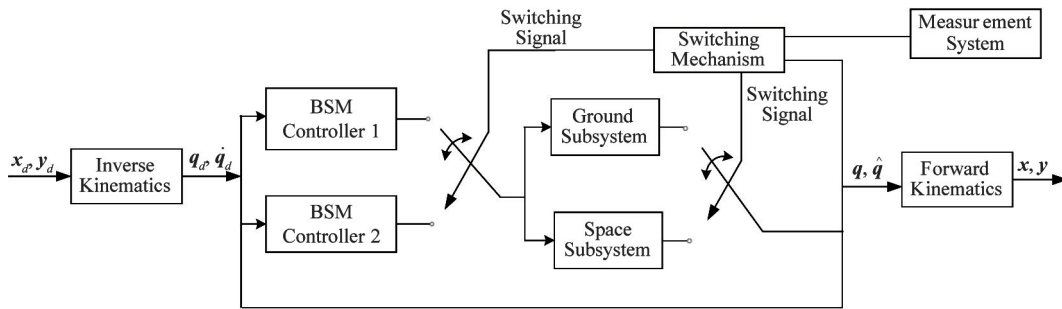


Fig. 2 Architecture diagram of SBSMC for space manipulator

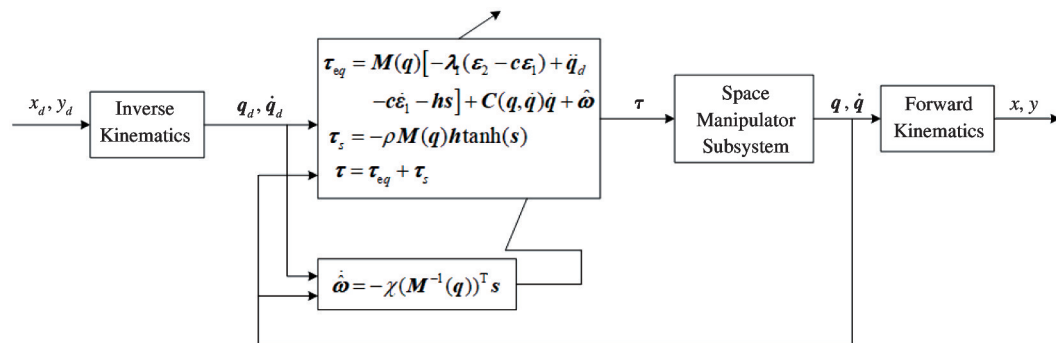


Fig. 3 Architecture diagram of BSM controller for space manipulator subsystem

3 Stability analysis

According to the theory of multi-Lyapunov function, the first thing is to make sure the stability of i th subsystem.

By substituting Eqs(29) and (30) into Eq. (27),

yields

$$\begin{aligned} \dot{V}_i &= \boldsymbol{\varepsilon}_1^T \boldsymbol{\varepsilon}_2 - \boldsymbol{\varepsilon}_1^T \mathbf{c} \boldsymbol{\varepsilon}_1 - \mathbf{s}^T \mathbf{h} \mathbf{s} - \rho \mathbf{s}^T \mathbf{h} \tanh(\mathbf{s}) \\ &= \boldsymbol{\varepsilon}_1^T \boldsymbol{\varepsilon}_2 - \boldsymbol{\varepsilon}_1^T \mathbf{c} \boldsymbol{\varepsilon}_1 - \mathbf{s}^T \mathbf{h} \mathbf{s} - \sum_{j=1}^n \sum_{i=1}^n \rho h_{ij} s_i \tanh(s_i) \end{aligned} \quad (32)$$

Let

$$\Phi = \begin{bmatrix} \mathbf{c} + \lambda_1^T \mathbf{h} \lambda_1 & \mathbf{h} \lambda_1 - \frac{1}{2} \mathbf{I} \\ \mathbf{h} \lambda_1 - \frac{1}{2} \mathbf{I} & \mathbf{h} \end{bmatrix} \quad (33)$$

accordingly,

$$\|\Phi\| = \mathbf{h}(\mathbf{c} + \lambda_1) - \frac{1}{4} \quad (34)$$

Denote $\boldsymbol{\varepsilon} = [\boldsymbol{\varepsilon}_1 \quad \boldsymbol{\varepsilon}_2]^T$, one can get

$$\begin{aligned} \boldsymbol{\varepsilon}^T \Phi \boldsymbol{\varepsilon} &= [\boldsymbol{\varepsilon}_1 \quad \boldsymbol{\varepsilon}_2] \begin{bmatrix} \mathbf{c} + \lambda_1^T \mathbf{h} \lambda_1 & \mathbf{h} \lambda_1 - \frac{1}{2} \mathbf{I} \\ \mathbf{h} \lambda_1 - \frac{1}{2} \mathbf{I} & \mathbf{h} \end{bmatrix} \begin{bmatrix} \boldsymbol{\varepsilon}_1 \\ \boldsymbol{\varepsilon}_2 \end{bmatrix} \\ &= \boldsymbol{\varepsilon}_1^T \mathbf{c} \boldsymbol{\varepsilon}_1 - \boldsymbol{\varepsilon}_1^T \boldsymbol{\varepsilon}_2 + (\lambda_1 \boldsymbol{\varepsilon}_1 + \boldsymbol{\varepsilon}_2)^T \mathbf{h} (\lambda_1 \boldsymbol{\varepsilon}_1 + \boldsymbol{\varepsilon}_2) \\ &= \boldsymbol{\varepsilon}_1^T \mathbf{c} \boldsymbol{\varepsilon}_1 - \boldsymbol{\varepsilon}_1^T \boldsymbol{\varepsilon}_2 + \mathbf{s}^T \mathbf{h} \mathbf{s} \end{aligned} \quad (35)$$

Then, Eq. (32) can be rewritten as

$$\dot{V}_i = -\boldsymbol{\varepsilon}^T \Phi \boldsymbol{\varepsilon} - \sum_{j=1}^n \sum_{i=1}^n \rho h_{ij} s_i \tanh(s_i) \quad (36)$$

For the first term on the right side of Eq. (36), it is clear from Eq. (33) that the positive definiteness of Φ can be guaranteed by choosing appropriate parameters \mathbf{h} , \mathbf{c} and λ_1 . For the second term, it can be learnt from Eq. (31) that $s_i \tanh(s_i) \geq 0$. What's more, ρ is a positive constant and \mathbf{h} is a positive definite matrix. Then $\dot{V}_i \leq 0$ in Eq. (36) can be guaranteed, that is, the i th subsystem is stable asymptotically.

The next step is to discuss the stability of the switching system. Assume that there are a_i , b_i and c_i (all of them are constants) in each subsystem.

By using Eqs(9), (16) in Eq. (21), it is easy to know that

$$a_i \|\boldsymbol{\varepsilon}\|^2 \leq V_i \leq b_i \|\boldsymbol{\varepsilon}\|^2 \quad (37)$$

then

$$\|\boldsymbol{\varepsilon}\|^2 \leq \frac{V_i}{a_i} \quad (38)$$

Based on Eq. (36), the following inequality can be derived

$$\dot{V}_i \leq -c_i \|\boldsymbol{\varepsilon}\|^2 \quad (39)$$

According to Eq. (38) and Eq. (39), the following inequality holds

$$\dot{V}_i \leq -\frac{c_i}{a_i} V_i \quad (40)$$

that is

$$\dot{V}_i \leq -\mu_i V_i, \mu_i = \frac{c_i}{a_i} \quad (41)$$

Let $\sigma(t) = i, \forall t \in [t_0, t_0 + \tau]$, where $\sigma(t)$ remarks the switching signal and τ is a positive constant, then

$$V_i(x(t_0 + \tau)) \leq e^{-\mu_i \tau} V_i(x(t_0)) \quad (42)$$

It is assumed that $(x(t_0), \sigma(t_0)) = (x_0, 1)$ is the initial state of system, t_1 and t_2 denote the switch-

ing time, $\sigma(t_1^+) = 2, \sigma(t_2^+) = 1, t_1 - t_0 \geq \tau, t_2 - t_1 \geq \tau$.

According to Eqs(37), (42) and the above assumption, the following inequality can be obtained:

$$V_2(t_1) \leq \frac{b_2}{a_1} V_1(t_1) \leq \frac{b_2}{a_1} e^{-\mu_1 \tau} V_1(t_0) \quad (43)$$

Further

$$\begin{aligned} V_1(t_2) &\leq \frac{b_1}{a_2} V_2(t_2) \leq \frac{b_1}{a_2} e^{-\mu_2 \tau} V_2(t_1) \\ &\leq \frac{b_1 b_2}{a_1 a_2} e^{-(\mu_1 + \mu_2) \tau} V_1(t_0) \end{aligned} \quad (44)$$

It can be deduced from Eq. (44) that $V_1(t_2) \leq V_1(t_0)$ so long as τ is large enough. On the basis of stability theory of multi-Lyapunov functions, the nonlinear switching scheme applied in this paper is stable globally and asymptotically.

4 Simulations

For the purpose of checking the capabilities of SB-SMC for space manipulator under gravity-varying conditions, a set of simulations are conducted with Matlab. For more intuitive comparison, simulation results of PD control for space manipulator are also exhibited. The parameters of space manipulator are shown in Table 1. The parameters of PD controller are set to be

$$\mathbf{K}_p = \text{diag}\{250, 250\}, \mathbf{K}_v = \text{diag}\{25, 25\} \quad (45)$$

and the desired trajectory for space manipulator is given as

$$\begin{cases} \mathbf{x}_d = 0.28 \cos \frac{\pi t}{5} + 0.85 \\ \mathbf{y}_d = 0.28 \sin \frac{\pi t}{5} \end{cases} \quad (46)$$

Table 1 Parameters of 2-DOF space manipulator

| Member | a_i/m | b_i/m | m_i/kg | $I_i/\text{kg} \cdot \text{m}^2$ |
|--------|----------------|----------------|-----------------|----------------------------------|
| Base | | 0.5 | 40 | 6.667 |
| Link1 | 0.5 | 0.5 | 4 | 0.333 |
| Link2 | 0.5 | 0.5 | 3 | 0.250 |

4.1 PD control for space manipulator

Fig. 4 and Fig. 5 show the tracking performance of the space manipulator with gravity-compensated PD controller in both cases. The PD controller is formed as

$$\boldsymbol{\tau} = \mathbf{K}_p \mathbf{e} + \mathbf{K}_v \dot{\mathbf{e}} + \mathbf{T}_f + \mathbf{G} \quad (47)$$

Based on Fig. 4, it is obvious that by employing PD controller with gravity compensation, the space manipulator performs a good behavior of trajectory tracking both in end-effector and two joints. However, this kind of PD controller is not appropriate for the manipu-

lator in the space, as it is shown in Fig. 5, which reflects the limitation of using the same PD controller in

the microgravity environment.

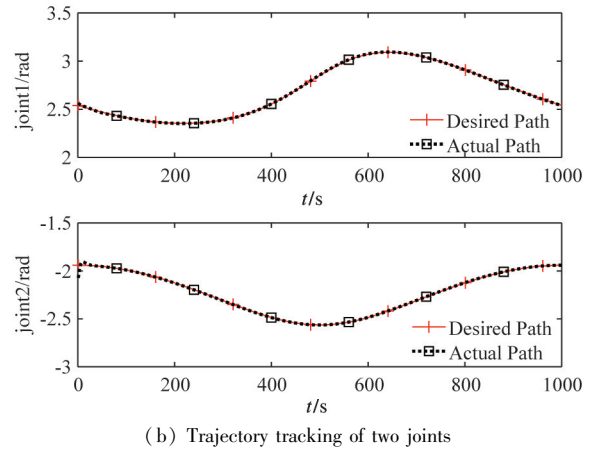
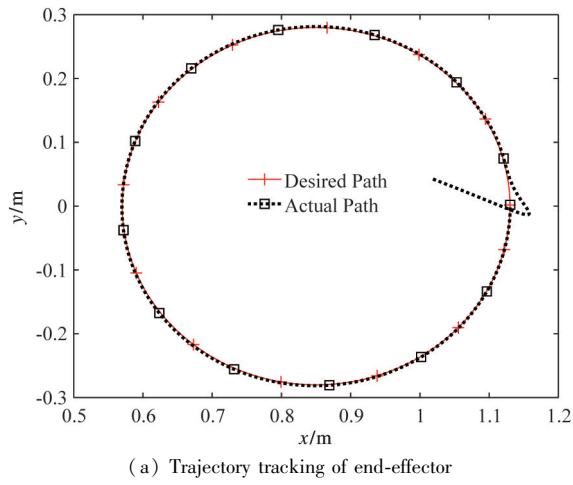


Fig. 4 Simulation results in gravity environment

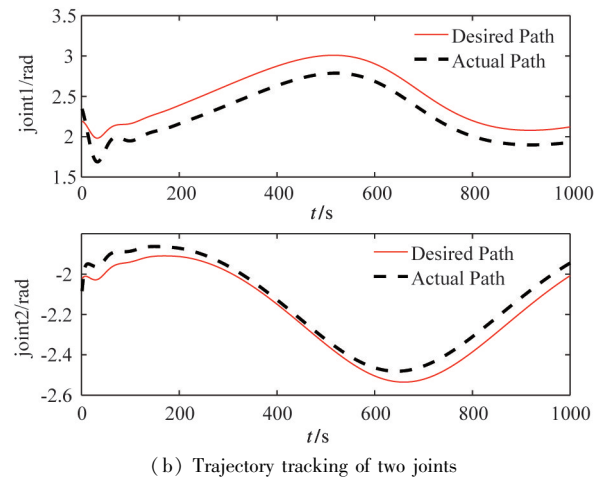
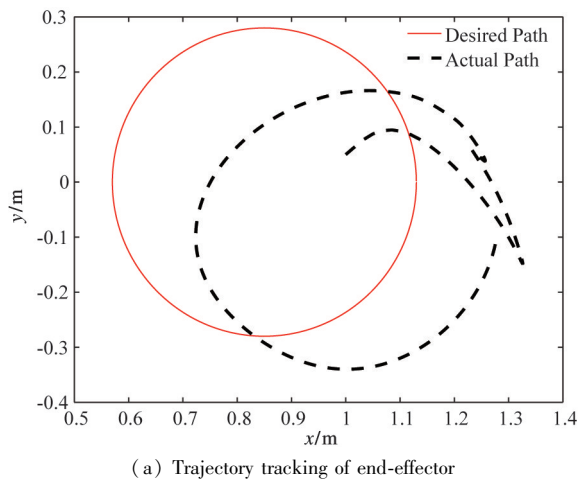


Fig. 5 Simulation results in microgravity environment

Fig. 6 and Fig. 7 depict the results of trajectory tracking for the space manipulator by applying the PD controller without gravity compensation under two con-

ditions. The PD controller is described as

$$\tau = K_p e + K_v \dot{e} + T_f \tag{48}$$

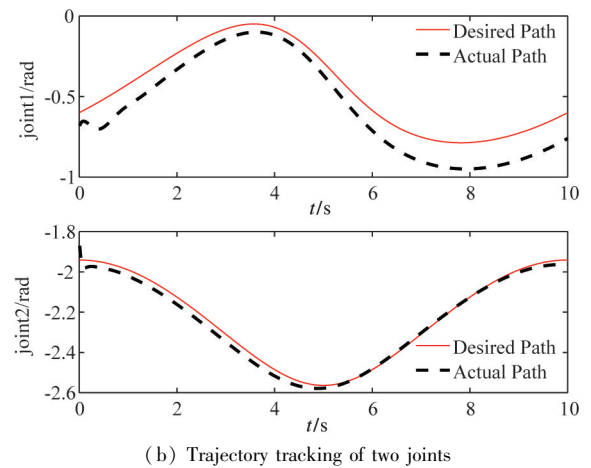
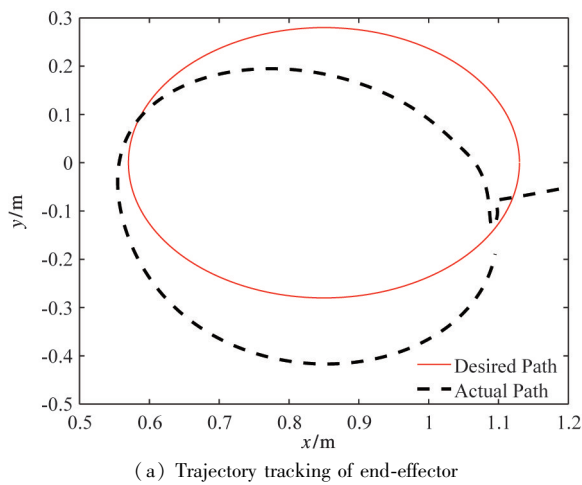
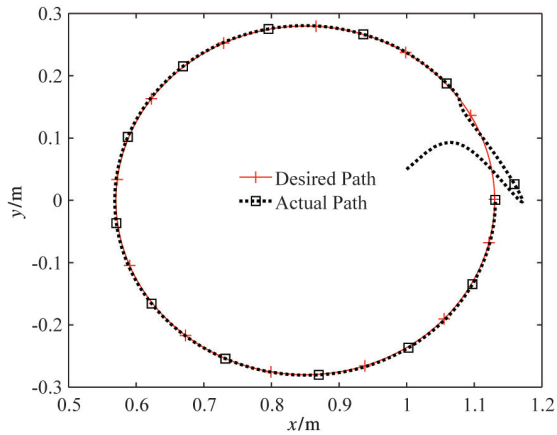
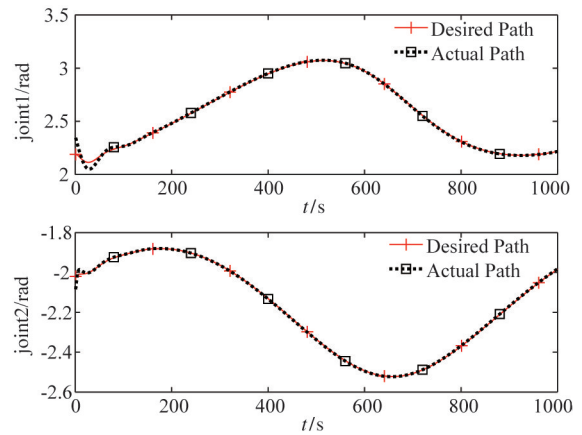


Fig. 6 Simulation results in gravity environment



(a) Trajectory tracking of end-effector



(b) Trajectory tracking of two joints

Fig. 7 Simulation results in microgravity environment

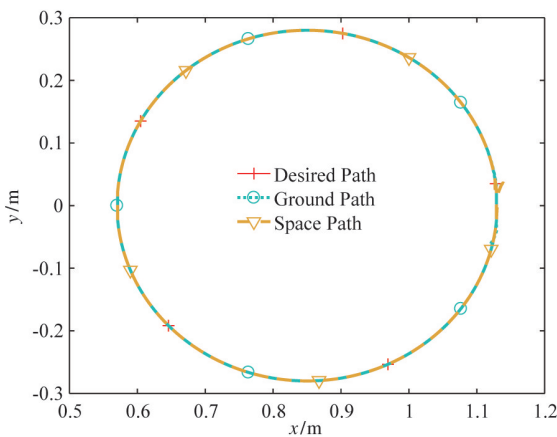
As it can be noticed in Fig. 7 that PD controller without gravity compensation is perfectly adequate for the trajectory tracking of space manipulator in the space. Nevertheless, the results provided in Fig. 6 indicate that this controller cannot meet the control requirements for space manipulator on the ground.

4.2 SBSMC for space manipulator

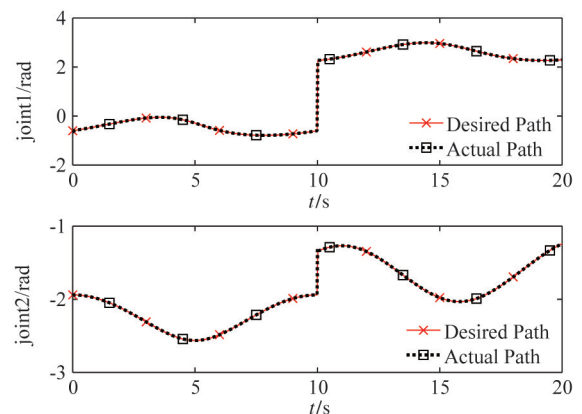
At the beginning of this simulation, the ground subsystem and its BSM controller are activated. Assuming that the measuring system of gravitational acceleration detects the acceleration $\leq 10^{-4} g$ at 10, then the control system switches to the space subsystem automatically, meanwhile, the space controller substitutes for the ground one. The simulation results are presented in Fig. 8.

As it can be noted in Fig. 8(a) and Fig. 8(b), the SBSMC approach guarantees the continuity of trajectory following in end-effector and two joints of the space manipulator despite changes in the control environments, which verifies that SBSMC is more effective and more robust than PD control in subsection 4.1 for

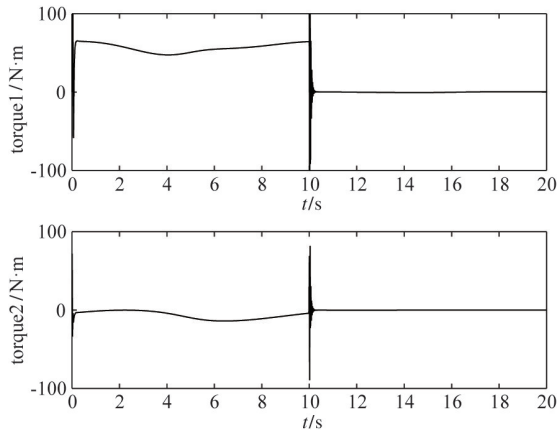
space manipulator confronted with gravity variation. It can be noticed that the joint angles vary largely at 10 in Fig. 8(b), this is because, when the system is in the free-floating state, the movement of the entire system increases 6-DOF, which makes the posture of the joint angles of the space manipulator different from that on the ground. The torques exerted on two joints are also presented in Fig. 8(c) to show the stability and continuity of controlling on the space manipulator in two phases. Furthermore, it can be observed from the curves of torques that the disturbance resulting from the switching between two subsystems disappears quickly as a result of the switch of their corresponding controllers. The reason why the torques vary largely at 10 is that there is no gravity term in the control law for the manipulator system in the space compared with the situation that the space manipulator is on the ground. Fig. 8(d) shows that in both periods, the tracking error maintains close to zero and the switching has no considerable effects on the tracking error of the space manipulator, except from transient vibration occurring at 10.



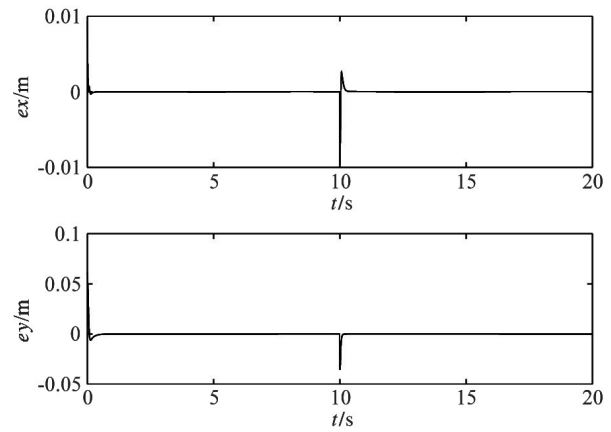
(a) Trajectory tracking of end-effector



(b) Trajectory tracking of two joints



(c) Control torque of two joints



(d) Tracking error of two joints

Fig. 8 Simulation results of SBSMC

5 Conclusion

The main contribution of this paper is that a SBSMC methodology is developed for space manipulator to handle the trajectory tracking issue derived from the transformation of gravity environments. This research combines the merits of switching control, backstepping control and sliding mode control. Different kinds of BSM controllers are designed for two subsystems while switching mechanism is formulated to accomplish the switching between two subsystems as well as their corresponding controllers. Compared with the control strategy that the same PD controller is applied to the space manipulator at two stages, the control strategy described in this paper provides great flexibility for the space manipulator under varying gravity conditions and achieves better tracking performance. It is worth considering, however, that the behaviors of space manipulator are constrained by many factors, such as links flexibility and hinge clearance, which will be the directions of future work.

Reference

- [1] Hu Q, Zhang J. Maneuver and vibration control of flexible manipulators using variable-speed control moment gyros[J]. *Acta Astronautica*, 2015, 113: 105-119
- [2] Dreyer M. The drop tower Bremen[J]. *Microgravity Science & Technology*, 2010, 22(4): 461-461
- [3] Sawada H, Ui K, Mori M, et al. Micro-gravity experiment of a space robotic arm using parabolic flight[J]. *Advanced Robotics*, 2004, 18(3): 247-267
- [4] Yoshida K. Experimental study on the dynamics and control of a space robot with experimental free-floating robot satellite simulators[J]. *Advanced Robotics*, 1994, 9(6): 583-602
- [5] Akin D L, Carignan C R. The reaction stabilization of on-orbit robots[J]. *Control Systems IEEE*, 2000, 20(6): 19-33
- [6] Fujii H, Uchiyama K, Yoneoka H, et al. Ground-based simulation of space manipulators using test bed with suspension system[J]. *Journal of Guidance Control & Dynamics*, 1996, 19(5): 985-991
- [7] Rybus T, Seweryn K, Oleś, Jakub, et al. Application of a planar air-bearing microgravity simulator for demonstration of operations required for an orbital capture with a manipulator[J]. *Acta Astronautica*, 2018, 155(1): 211-229
- [8] Song J, Yao D, Hu J, et al. A novel calibration system for a space manipulator[C] // Proceedings of IEEE/RSJ International Conference on Intelligent Robots & Systems, Beijing, China, 2006: 4672-4677
- [9] Yuan J, Zhu Z, Ming Z, et al. An innovative method for simulating microgravity effects through combining electromagnetic force and buoyancy[J]. *Advances in Space Research*, 2015, 56(2): 355-364
- [10] Wang W K. Simulation study on motion behavior of spacecraft mechanisms [J]. *Manned Spaceflight*, 2013(5): 63-70 (In Chinese)
- [11] Qin L, Liu F C, Ling L H, et al. Fuzzy adaptive robust control for space robot considering the effect of the gravity [J]. *Chinese Journal of Aeronautics*, 2014(6): 223-231
- [12] Qin L, Jia X J, Liu C F, et al. Friction compensation control of space manipulator considering the effects of gravity[C] // Proceedings of 35th Chinese Control Conference (CCC), Chengdu, China, 2016: 951-956
- [13] Sharma R, Bhasin S, Gaur P, et al. A switching-based collaborative fractional order fuzzy logic controllers for robotic manipulators[J]. *Applied Mathematical Modelling*, 2019, 73: 228-246
- [14] Bishop B E, Spong M W. Control of redundant manipulators using logic-based switching [C] // Proceedings of IEEE Conference on Decision & Control, Tampa, USA, 1998: 1488-1493
- [15] Xing X, Liu J. Switching fault-tolerant control of a moving vehicle-mounted flexible manipulator system with state constraints[J]. *Journal of the Franklin Institute*, 2018, 355(6): 3050-3078
- [16] Branicky M S. Multiple Lyapunov functions and other

- analysis tools for switched and hybrid systems[J]. *IEEE Transactions on Automatic Control*, 1998, 43(4): 475-482
- [17] Van M, Mavrouniotis M, Ge S S. An adaptive backstepping nonsingular fast terminal sliding mode control for robust fault tolerant control of robot manipulators [J]. *IEEE Transactions on Systems, Man, and Cybernetics: Systems*, 2019, 49(7): 1448-1458
- [18] Wang J, Xu F, Lu G D. A model weighted adaptive neural backstepping sliding-mode controller for cooperative manipulator system [J]. *International Journal of Advanced Robotic Systems*, 2017, 14(6): 1-14
- [19] Rodolfo G R, Vicente P V. Task-space neuro-sliding mode control of robot manipulators under Jacobian uncertainties[J]. *International Journal of Control Automation & Systems*, 2011, 9(5): 895-904
- [20] Papadopoulos E, Dubowsky S. On the nature of control algorithms for free-floating space manipulators[J]. *IEEE Transactions on Robotics & Automation*, 2002, 7(6): 750-758
- [21] Wöske, Florian, Kato T, Rievers B, et al. GRACE accelerometer calibration by high precision non-gravitational force modeling[J]. *Advances in Space Research*, 2019,

63(3): 1318-1335

Liu Fucai, born in 1966. He received the Ph. D degree from Department of Control Science and Engineering, School of Astronautics, Harbin Institute of Technology in 2003. He received the M. S. degree from the Department of Automation, Northeast Heavy Mechanism Academe, Qiqihar, China, in 1994. He is now a professor and doctoral supervisor of Department of Automation, School of Electrical Engineering, Yanshan University. He is also the director of Hebei Automation Experimental Teaching Demonstration Center. He has authored/co-authored more than 280 papers in mathematical, technical journals, and conferences. He is the author of the book ‘Fuzzy Model Identification for Nonlinear Systems and Its Applications’. His current research interests include spatial mechanism behavior analysis and control, stability analysis for fuzzy positive systems, fuzzy identification and control of nonlinear systems, etc.